NANO LETTERS

Letter

Selective Growth of Well-Aligned Semiconducting Single-Walled Carbon Nanotubes

Lei Ding, Alexander Tselev, Jinyong Wang, Dongning Yuan, Haibin Chu, Thomas P. McNicholas, Yan Li, and Jie Liu

Nano Lett., **Article ASAP** • DOI: 10.1021/nl803496s

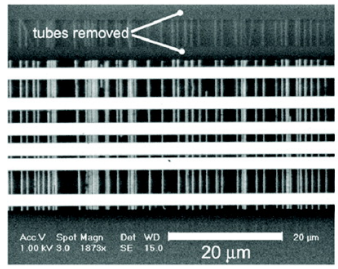

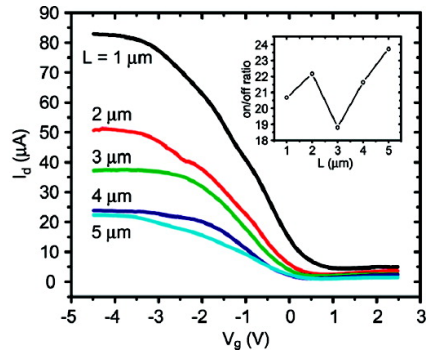

More About This Article

Additional resources and features associated with this article are available within the HTML version:

- Supporting Information
- Access to high resolution figures
- Links to articles and content related to this article
- Copyright permission to reproduce figures and/or text from this article

View the Full Text HTML

NANO LETTERS

XXXX
Vol. xx, No. x
-

Selective Growth of Well-Aligned Semiconducting Single-Walled Carbon Nanotubes

Lei Ding,[†] Alexander Tselev,[†] Jinyong Wang,[‡] Dongning Yuan,[†] Haibin Chu,[†,‡] Thomas P. McNicholas,[†] Yan Li,[*,‡] and Jie Liu[*,†]

Department of Chemistry, Duke University, Durham, North Carolina 27708, and Beijing National Laboratory for Molecular Sciences, Key Laboratory for the Physics and Chemistry of Nanodevices, National Laboratory of Rare Earth Material Chemistry and Application, College of Chemistry and Molecular Engineering, Peking University, Beijing 100871, China

Received November 18, 2008; Revised Manuscript Received December 17, 2008

ABSTRACT

High-density arrays of perfectly aligned single-walled carbon nanotubes (SWNTs) consisting almost exclusively of semiconducting nanotubes were grown on ST-cut single crystal quartz substrates. Raman spectroscopy together with electrical measurements of field effect transistors (FETs) fabricated from the as-grown samples showed that over 95% of the nanotubes in the arrays are semiconducting. The mechanism of selective growth was explored. It is proposed that introducing methanol in the growth process, combined with the interaction between the SWNTs and the quartz lattice, leads to the selective growth of aligned semiconducting nanotubes. Such a high density of horizontally aligned semiconducting SWNTs can be readily used in high current nanoFETs and sensors. This method demonstrates great promise to solve one of the most difficult problems which limits application of carbon nanotubes in nanoelectronics—the coexistence of metallic and semiconducting nanotubes in samples produced by most, if not all, growth methods.

Single-walled carbon nanotubes have shown outstanding potential in nanoelectronics due to their exceptional properties such as high mobility,[1] high thermal conductivity,[2] and good chemical[3] and mechanical stability.[4] The device performance was shown to be better than that of Si-based devices in some applications.[5] However, even though the devices made from individual nanotubes have shown outstanding performance,[1,2,6] the high hope for the next generation of carbon nanotube based electronics is hampered by several major problems. Among them are the lack of reliable methods to control the alignment and position of nanotubes as well as, and perhaps most importantly, simultaneous growth of nanotubes with different structures (chiralities), yielding random mixtures of metallic and semiconducting nanotubes.[7] Over the past decade, significant efforts in research have been focused on finding solutions to these problems but only limited progress has been made. For example, researchers have demonstrated the separation of metallic from semiconducting SWNTs based on electrophoresis,[8] physicochemical modification,[9,10] density gradient induced centrifugation,[11] selective elimination by electrical breakdown,[12] gas-phase plasma etching,[13] and several other methods.[14,15] However, the chemical separation methods used in these processes always introduce defects and contamination to the SWNTs. Additionally, the separated nanotubes still need to be assembled onto a substrate for device fabrication. Currently no reliable methods exist to accomplish this step. Therefore the direct growth of metallic and semiconducting SWNTs on suitable substrates would be a significant advancement toward their easy integration with existing Si fabrication technology.[16−22] According to these published papers, there is still some room to improve such as the ratio and alignment of the selectively grown SWNTs on surfaces. Nearly all the SWNTs of the selective samples were shown as random, which was thought to increase the overlap of the nanotubes and the resistance caused by the tube junctions. But the direct growth method was thought to be a significant approach for its advantages, such as high purity of nanotubes and the availability of methods to control the alignment of the nanotube during growth by electric field,[23] laminar gas flow,[24] and single crystal substrates.[25−27] Recently, uniform nanotube arrays fabricated on single crystal substrates[28,29] can be used directly as a thin film for making a large amount of devices—a major breakthrough in practical fabrication of nanotube devices. However, the coexistence of metallic and semiconducting

* Corresponding authors, j.liu@duke.edu and yanli@pku.edu.cn.
† Duke University.
‡ Peking University.

10.1021/nl803496s CCC: $40.75

nanotubes in such samples is still a problem hindering their immediate application.

Herein, we present a chemical vapor deposition (CVD) approach, which allows selective growth of high density arrays of well-aligned SWNTs with almost exclusively semiconducting SWNTs. The dense arrays of aligned SWNTs were grown on single-crystal ST-cut quartz substrates using an ethanol/methanol mixture as the carbon source and Cu nanoparticles as catalysts. Nanotubes within the arrays revealed a narrow diameter distribution from 1.55 to 1.78 nm with over 95% of nanotubes being semiconducting. We proved that the selective growth is a result of two crucial factors: the presence of methanol in the CVD process and a strong interaction (affinity) between SWNTs and the quartz lattice. The samples can be used for direct fabrication of nanotube FETs with good performances. Still, more work needs to be done to fully understand the growth mechanism and achieve reliable 100% selective growth of semiconducting nanotubes. However, the fact that such highly selective growth of well-aligned semiconducting nanotubes can be achieved represents a promise for solving the last major problem that is limiting the wide use of nanotubes in nanoelectronics. To the best of our knowledge, this is the first time that the control of horizontal alignment and the control of electronic properties can be achieved simultaneously.

In our experiments, a 1.0 mM $CuCl_2$/poly(vinylpyrrolidone) alcohol solution was used to deposit catalyst on to the substrate. The catalyst patterning and growth processes were similar to the method reported previously except for the addition of a methanol bubbler.[29] Typically, ST-cut (36° Y-cut) single crystal quartz was used as the substrate for the SWNT growth unless otherwise specified. Other substrates including SiO_x, *Z*-cut single crystal quartz, and 42° *Y*-cut single crystal quartz were also used in this study to help elucidate the growth mechanism. The growth experiments were performed in a 1 in. tube furnace at 900 °C. The substrate with catalyst precursor deposited on it was treated with oxygen plasma for 15 min to remove the poly(vinylpyrrolidone) in the catalyst precursor. Then the substrate was heated up to 800 °C and kept for 15 min with a flow of hydrogen (500 sccm), followed by CVD growth of SWNTs at 900 °C. Although the types of nanotubes grown under different ethanol/methanol ratios are not the same, typically, a flow of hydrogen (450 sccm) and argon (150 sccm through an ethanol bubbler and 300 sccm through a methanol bubbler) was used for the growth of semiconducting SWNTs. After 15 min of growth, the sample was cooled to room temperature and inspected with scanning electron microscopy (SEM), atomic force microscopy (AFM), and a Raman spectrometer. A mixture of metallic and semiconducting SWNTs can be obtained at different growth conditions on the same type of substrate.

Resonant Raman spectroscopy (RRS) has been used to characterize the samples. RRS has been proven to be a powerful tool for characterizing and revealing the detailed structure and the electronic and phonon properties of SWNTs. The radial breathing mode (RBM) and G-band features of

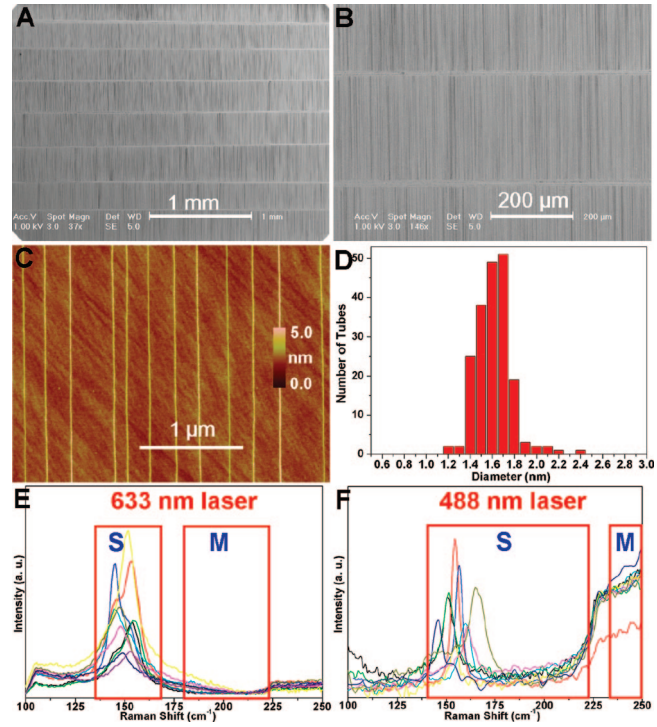

Figure 1. Arrays of almost exclusively semiconducting SWNTs. (A and B) SEM images. The bright and parallel horizontal lines visible in the images are catalyst lines. (C) AFM image. (D) Diameter distribution of 200 SWNTs of an array measured by AFM. (E and F) Raman spectra of SWNTs transferred onto the SiO_x/Si substrates. The spectra were obtained using 488 and 633 nm excitation laser lines at 10 different spots over the substrate for each laser line. Each curve in a panel shows a spectrum at a spot on the substrate. Peaks within the rectangles marked with S correspond to the semiconducting SWNTs. The rectangles marked with M denote the frequency range where RBM peaks of metallic SWNTs are expected.

Raman spectra can be used to assign and distinguish the semiconducting and metallic SWNTs, especially when multiple excitation lasers are used. In our experiment, lasers with three different wavelengths of 488, 633, and 785 nm were used to distinguish the semiconducting and metallic SWNTs sufficiently for our samples. More than 10 spots on each sample were characterized by RRS. In order to avoid the influence of the Raman peaks from the quartz substrates at 127 and 205 cm^{-1}, the SWNTs grown on ST-cut quartz were transferred onto the SiO_x/Si for RRS characterization (see Figure S1 in Supporting Information).

Figure 1 presents the scanning electron microscopy (SEM) and atomic force microscopy (AFM) images and Raman spectra of the aligned semiconducting SWNTs. The uniform, high-density and perfectly aligned arrays of long nanotubes can be found on the entire ST-cut quartz substrate from SEM images. AFM measurements show that the nanotubes in the array have a narrow diameter distribution from 1.4 to 1.8 nm with an average diameter of 1.65 nm (Figure 1, panels C and D). The substrate surface is remarkably clean and free of amorphous carbon contamination. A high fraction of the semiconducting tubes in the arrays becomes evident from RRS data. Raman spectra recorded with 633 and 488 nm excitation lines (Figure 1, panels E and F), show a narrow

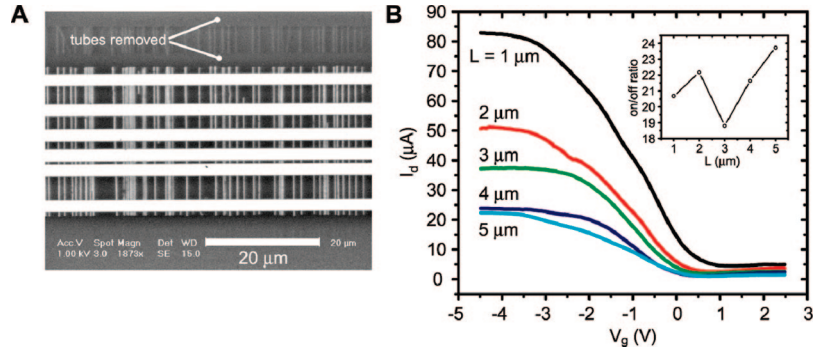

Figure 2. High on/off ratio FETs fabricated with as-grown aligned CNT arrays top-gated by solid electrolyte polymer films. (A) Large magnification view of the set of electrodes of a test device. The widths of the gaps between the 40 nm thick gold contact lines correspond to the channel lengths of FETs (from top to bottom): 4, 3, 2, 1, and 5 μm. To break possible current paths through the nanotube array past the transistor channels, the tubes were partially removed by reactive ion etching (RIE) in oxygen plasma. (B) Family of transfer characteristics (drain current, I_d, vs top gate voltage, V_g) of one of the test devices under a bias voltage $V_{ds} = 80$ mV. The parameter of the family is the transistor channel length L. The channel width is 0.5 mm. (Inset) The on/off ratios obtained for the device as a function of the channel length, L.

distribution of RBM frequencies between 143 and 158 cm^{-1}. Notably, no peaks are visible in the range, where RBM peaks of metallic tubes are expected from the so-called Kataura plot[30] as highlighted in the figures with red rectangles. From the experimental relationship between a SWNT diameter d (in nm) and a RBM shift ω (in cm^{-1}), $\omega = 248/d$,[30] we estimated that the diameters of SWNTs range from 1.55 to 1.78 nm, which is narrower than that measured by AFM. It is possible that the deformation of SWNTs due to the force produced by the tip during AFM measurements leads to the apparent broadening of the diameter distribution. No RBM peaks have been found when a 785 nm laser was used for excitation, which further supports a low percentage of metallic SWNTs since no Raman peaks from semiconducting nanotubes are expected in the case of the 785 nm excitation laser because the diameter of the semiconducting nanotubes with resonance at this excitation line needs to be smaller ($<$1.13 nm) than that existing in our sample. The enhanced yield of semiconducting SWNTs is supported by the analyses of the G-band features of the Raman spectra (see Figure S2 in Supporting Information). Further, Raman spectra obtained from as-grown samples on quartz substrates are similar to those measured on arrays transferred onto SiO_x/Si substrates (see Figure S3 in Supporting Information). The spectroscopic details over the disorder band (D-band) reveal the low defect density on the SWNTs (see Figure S4 in Supporting Information).

To further confirm a high percentage of semiconducting nanotubes in these SWNT arrays, we performed electrical characterization of the FETs fabricated from as-grown aligned nanotube arrays directly on quartz substrates. The FETs were fabricated with a top gate using standard e-beam lithography and utilizing a solid conducting polymer (poly(ethylene oxide)/lithium perchlorate mixture (PEO:$LiClO_4$•$3H_2O$)) as the top gate following previously reported methods.[31,32] Each test device consisted of five transistors fabricated along one set of parallel nanotubes with channel length L from 1 to 5 μm as illustrated in Figure 2A. The channel width of FETs was 500 μm, meaning the number of nanotubes spanning across each device is at least 500. The drain leakage current due to the gate voltage did not exceed 20 nA at $V_g = 4.5$ V with approximately linear dependence on the gate voltage. Consequently, the contribution of this part of the leakage current in the off-state response of the transistors did not exceed 5%. The drain leakage current associated with the bias voltage was in the picoampere range and can be ignored in the calculation. More detailed description on the test device configuration, fabrication, and electrical properties can be found in the Supporting Information (see Figures S5 and S6 in Supporting Information). We have measured altogether six such 5-fold devices fabricated at different spots across the chip and found that the on/off ratios normally fall in the range between 18 and 32 with some FETs showing higher ratios up to 85 (see Figure S7 in Supporting Information). Figure 2B displays the family of transfer characteristics of one of these devices with the channel length as a parameter. Since the number of parallel nanotubes in each device is over 500, the on/off ratios measured here represent the average ratio of semiconducting and metallic nanotubes in the samples.

The on/off ratios in all the measured devices are significantly larger than 3, which is the expected value for SWNT nanotube networks with no selectivity in growth, where all chiralities of nanotubes appear in equal probability, yielding 1/3 of species being metallic. This observation clearly indicates that a large fraction the nanotubes in the as-grown array are semiconducting. In particular, the on/off ratio of 20 is expected if 95% of tubes are semiconducting assuming all nanotubes have similar resistances in their ON-state.[7] We have estimated from these measurements that the samples consisted of 95−98% semiconducting nanotubes.

In the selective growth of semiconducting SWNTs, two factors were found to be essential. First is the introduction of methanol in the growth. Our previous work showed that SWNTs have an average diameter of 1.2 nm,[29] and others showed that the ratio of metallic SWNTs is about 1/3 when only ethanol is used as the carbon feeding gas for the growth on ST-cut quartz.[28] We observed that the introduction of methanol in the growth leads to the changes in diameters and in the semiconducting/metallic ratio of the SWNTs. In

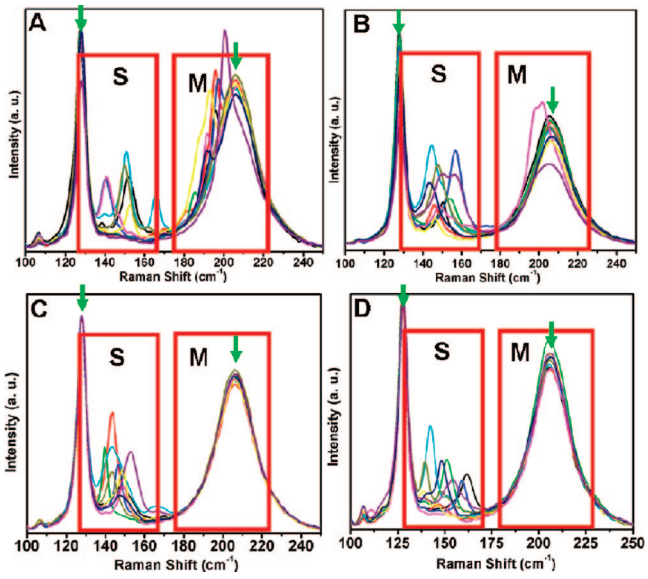

Figure 3. Raman spectra showing RBMs of as-prepared SWNTs on ST-cut quartz with different methanol/ethanol ratios. The flow rate of ethanol was set as 150 sccm, and the flow rate of methanol was (A) 0 sccm, (B) 150 sccm, (C) 450 sccm, and (D) 600 sccm, respectively. The Raman spectra was recorded with an excitation laser line of 633 nm. Ten different spots of each sample were characterized on the whole surface. Each curve in a panel shows a spectrum at a spot on the substrate. The sharp peaks at 127 cm^{-1} and the broad peaks at 205 cm^{-1}, marked with green arrows, correspond to the Raman spectra of the quartz. Peaks marked with S within the rectangles correspond to the semiconducting SWNTs. The rectangles marked with M denote the frequency range where RBM peaks of metallic SWNTs are expected.

order to understand the role of methanol in the growth process, we tried the growth of SWNTs with different ratios of methanol/ethanol as the carbon feeding gas at the same growth temperature. We set the flow rate of ethanol at 150 sccm and varied the flow rate of methanol to tune the methanol/ethanol ratios; a flow of 450 sccm hydrogen was used in the growth. Interestingly, it was found that no SWNTs were synthesized on the surface when only methanol was used as the carbon feeding gas. We believe that this is the result of the high decomposition temperature of methanol.[33] Previous work demonstrated that the carbonization temperature increases with the increasing hydrogen-to-carbon ratio in the hydrocarbon CVD process.[34] Thus, a much higher temperature should be used to decompose methanol for the growth of SWNTs. Though methanol cannot be used as the only carbon feeding gas for the growth of SWNTs under our growth conditions, the selectivity was enhanced with the increasing ratios of methanol/ethanol during growth. Figure 3 presents the Raman spectra of SWNTs grown with different methanol/ethanol ratios by the same growth conditions. The spectroscopic details of the RBM peaks shown in Figure 3A indicate the existence of a significant amount of metallic SWNTs on the surface when only ethanol was used as the carbon feeding gas. Two metallic RBM peaks at 198 and 201 cm^{-1} have been found in Figure 3B with the introduction of 150 sccm methanol in the growth. No metallic peaks have been found in Figure 3C and Figure 3D when the flow rates of methanol were increased to 450 and 600 sccm, respectively. The 785 nm excitation line has also been used to characterize the Raman spectra of the SWNTs in Figure 3, panels C and D. No RBM peaks were found when a 785 nm laser was used for excitation, which further supports a low percentage of metallic SWNTs in our sample. The sharp peaks at 127 cm^{-1} and the broad peaks at 205 cm^{-1}, marked with green arrows in (Figure 3, panels D, F, and H), correspond to the Raman signals from quartz. The results indicated that the methanol/ethanol ratio can affect the growth selectivity. We explain the enhanced selectivity by methanol as the following. At our growth temperature of 900 °C, even though methanol cannot produce nanotubes, we believe that the OH radical from methanol can selectively etch metallic SWNTs because of their smaller ionization potential as compared to semiconducting ones.[35] This selective etching would result in the enrichment of semiconducting SWNTs found in our samples. Also, the etching effect of the OH radicals prevents the formation of amorphous carbon on the

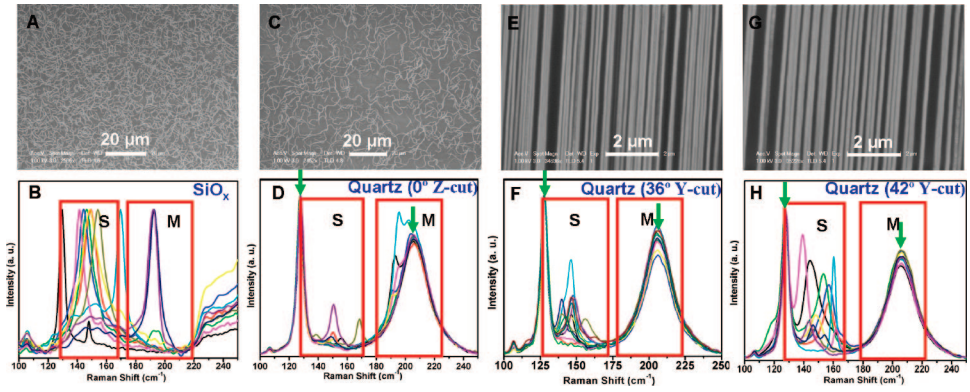

Figure 4. SEM images and Raman spectra showing RBMs of as-prepared SWNTs on (A and B) SiO_x, (C and D) 0° *Z*-cut quartz, (E and F) 36° *Y*-cut quartz, and (G and H) 42° *Y*-cut quartz, respectively. All the SWNTs on these wafers were grown under the same conditions. The Raman spectra was recorded with an excitation laser line of 633 nm. Ten different spots of each sample were characterized on the whole surface. Each curve in a panel shows spectrum at a spot on the substrate. The sharp peaks at 127 cm^{-1} and the broad peaks at 205 cm^{-1}, marked with green arrows in (D, F, and H), correspond to the Raman spectra of the quartz. Peaks marked with S within the rectangles correspond to the semiconducting SWNTs. The rectangles marked with M denote the frequency range where RBM peaks of metallic SWNTs are expected.

surface, making the surface clean as confirmed by our AFM images.

The second important factor for the selective growth is the quartz substrate. We found that on noncrystalline substrates and *Z*-cut single crystal quartz wafer under the same growth conditions, a mixture of metallic and semiconducting nanotubes was grown with no indication of selective growth of semiconducting nanotubes. Figure 4 presents the SEM images and Raman spectra of SWNTs grown on different substrates with the same growth conditions. Random SWNTs were found on SiO_x and *Z*-cut quartz surfaces, while well-aligned SWNT arrays can be grown on 36° and 42° *Y*-cut quartz surfaces. It was believed that the linear lattices on *Y*-cut quartz guide the alignment of SWNTs. Also, it was found that the selectivity can be affected by the substrate. The spectroscopic details of the RBM peaks shown in Figure 4B and Figure 4D indicate the existence of a significant amount of metallic SWNTs on the surface, while no metallic peaks are found in Figure 4F and Figure 4H. The 785 nm excitation line has also been used to characterize the Raman spectra of the SWNTs on *Y*-cut quartz, and no RBM peaks have been found, which further supports a low percentage of metallic SWNTs in our sample. The results indicated that the substrate can affect the growth selectivity. On the basis of these observations, we believe that the *Y*-cut quartz lattice on the surface is critical for the enrichment of well-aligned, long, and semiconducting SWNTs. Previous work shows evidence that SWNTs stick to the quartz surface during growth.[29] The interaction between the lattice of substrate and the SWNTs guides the alignment of SWNTs on the surface.[36] Our recent results show that the introduction of methanol during growth can increase the interaction between the *Y*-cut quartz lattices and the SWNTs. The obvious blue shifts of G-bands, caused by the strong interaction between the lattice and the SWNT, can be found on the samples when the flow rate of methanol was up to 450 sccm. No blue shifts of G-bands have been found on SWNTs grown on SiO_x and *Z*-cut quartz wafer under the same growth condition, which indicate a relatively weak interaction between the substrate and the SWNTs. It is believed that the interaction between the lattice and SWNT was critical to the selective growth. The semiconducting SWNTs with diameters between 1.5 and 1.8 nm should match well with the atomic spacing in the *Y*-cut quartz lattice. Ultimately, it was found that semiconducting SWNTs were enriched with the introduction of methanol in the growth. Additionally, even when ST (36° *Y*)-cut quartz substrates were used, the RBM peaks of SWNTs grown within the catalyst regions show a relatively wider diameter distribution, worse alignment, and existence of metallic nanotubes (see Figure S8 in Supporting Information). These observations indicate that the selective growth only applies to the aligned nanotubes with a very narrow diameter distribution. The single crystal quartz substrate is critical for the growth of aligned nanotubes with narrow diameter distribution, together with the contribution of the right growth conditions. Additional experimental and theoretical work designed to fully understand the molecular origin of this selective growth is currently underway.

In summary, we have discovered a method to grow high-density, perfectly aligned SWNT arrays with a significantly enhanced fraction of semiconducting SWNTs on ST-cut quartz using an ethanol/methanol mixture. AFM, RRS, and electrical testing of the FETs fabricated from the arrays demonstrate the uniformity of SWNTs in alignment, diameter, and electronic properties. It is also evident that the growth selectivity can be attributed to the combination of introducing methanol in the growth process and using ST-cut quartz as the substrate. The samples can be directly utilized for the fabrication of large amounts of FETs with standard photolithography or e-beam lithography. It is much more suitable to be adapted by the current Si fabrication technology due to the uniformity of the sample and the perfect alignment of the nanotubes. We believe that these results represent important progress toward the ability to simultaneously control the types of nanotubes as well as their alignment. It is widely accepted that the lack of such control is the last major problem for the wide application of carbon nanotubes in electronics.

Acknowledgment. The work is supported in part by a grant from NRL (N00173-04-1-G902), funding from Duke University, and support from Unidym, Inc. Y.L. acknowledges financial support of NSF (Projects 50772002 and 90406018) and MOST (Projects 2006CB932403, 2007CB936202, and 2006CB932701) of China. The authors also acknowledge helpful discussions with Dr. Chenguang Lu at Columbia University.

Supporting Information Available: More detailed experimental conditions and methods for device fabrication. This material is free of charge via the Internet at http://pubs.acs.org.

References

(1) Javey, A.; Kim, H.; Brink, M.; Wang, Q.; Ural, A.; Guo, J.; McIntyre, P.; McEuen, P.; Lundstrom, M.; Dai, H. J. *Nat. Mater.* **2002**, *1*, 241.
(2) Pop, E.; Mann, D.; Wang, Q.; Goodson, K.; Dai, H. J. *Nano Lett.* **2006**, *6*, 96.
(3) Dresselhaus, M. S.; Dresselhaus, G.; Eklund, P. C. *Science of fullerenes and carbon nanotubes*; Academic Press: San Diego, 1996.
(4) Saito, R.; Dresselhaus, G.; Dresselhaus, M. S. *Physical Properties of Carbon Nanotubes*; Imperial College Press: London, 1998.
(5) Appenzeller, J.; Martel, R.; Derycke, V.; Radosavjevic, M.; Wind, S.; Neumayer, D.; Avouris, P. *Microelectron. Eng.* **2002**, *64*, 391.
(6) Tans, S. J.; Verschueren, A. R. M.; Dekker, C. *Nature* **1998**, *393*, 49.
(7) Kim, W.; Choi, H. C.; Shim, M.; Li, Y. M.; Wang, D. W.; Dai, H. J. *Nano Lett.* **2002**, *2*, 703.
(8) Krupke, R.; Hennrich, F.; von Lohneysen, H.; Kappes, M. M. *Science* **2003**, *301*, 344.
(9) Chattopadhyay, D.; Galeska, L.; Papadimitrakopoulos, F. *J. Am. Chem. Soc.* **2003**, *125*, 3370.
(10) Chen, Z. H.; Du, X.; Du, M. H.; Rancken, C. D.; Cheng, H. P.; Rinzler, A. G. *Nano Lett.* **2003**, *3*, 1245.
(11) Arnold, M. S.; Green, A. A.; Hulvat, J. F.; Stupp, S. I.; Hersam, M. C. *Nat. Nanotechnol.* **2006**, *1*, 60.
(12) Collins, P. C.; Arnold, M. S.; Avouris, P. *Science* **2001**, *292*, 706.
(13) Zhang, G. Y.; Qi, P. F.; Wang, X. R.; Lu, Y. R.; Li, X. L.; Tu, R.; Bangsaruntip, S.; Mann, D.; Zhang, L.; Dai, H. J. *Science* **2006**, *314*, 974.
(14) LeMieux, M. C.; Roberts, M.; Barman, S.; Jin, Y. W.; Kim, J. M.; Bao, Z. N. *Science* **2008**, *321*, 101.
(15) Dyke, C. A.; Stewart, M. P.; Tour, J. M. *J. Am. Chem. Soc.* **2005**, *127*, 4497.
(16) Li, Y. M.; Mann, D.; Rolandi, M.; Kim, W.; Ural, A.; Hung, S.; Javey, A.; Cao, J.; Wang, D. W.; Yenilmez, E.; Wang, Q.; Gibbons, J. F.; Nishi, Y.; Dai, H. J. *Nano Lett.* **2004**, *4*, 317.

(17) Bachilo, S. M.; Balzano, L.; Herrera, J. E.; Pompeo, F.; Resasco, D. E.; Weisman, R. B. *J. Am. Chem. Soc.* **2003**, *125*, 11186.
(18) Li, Y. M.; Peng, S.; Mann, D.; Cao, J.; Tu, R.; Cho, K. J.; Dai, H. J. *J. Phys. Chem. B* **2005**, *109*, 6968.
(19) Li, X. L.; Tu, X. M.; Zaric, S.; Welsher, K.; Seo, W. S.; Zhao, W.; Dai, H. J. *J. Am. Chem. Soc.* **2007**, *129*, 15770.
(20) Wang, B.; Poa, C. H. P.; Wei, L.; Li, L. J.; Yang, Y. H.; Chen, Y. *J. Am. Chem. Soc.* **2007**, *129*, 9014.
(21) Ciuparu, D.; Chen, Y.; Lim, S.; Haller, G. L.; Pfefferle, L. *J. Phys. Chem. B* **2004**, *108*, 503.
(22) Qu, L.; Du, F.; Dai, L. *Nano Lett.* **2008**, *8*, 2682.
(23) Ural, A.; Li, Y. M.; Dai, H. J. *Appl. Phys. Lett.* **2002**, *81*, 3464.
(24) Huang, S. M.; Maynor, B.; Cai, X. Y.; Liu, J. *Adv. Mater.* **2003**, *15*, 1651.
(25) Han, S.; Liu, X. L.; Zhou, C. W. *J. Am. Chem. Soc.* **2005**, *127*, 5294.
(26) Yuan, D.; Ding, L.; Chu, H.; Feng, Y.; McNicholas, T. P.; Liu, J. *Nano Lett.* **2008**, *8*, 2576.
(27) Zhou, W.; Rutherglen, C.; Bruke, P. J. *Nano Res.* **2008**, *1*, 158.
(28) Kang, S. J.; Kocabas, C.; Ozel, T.; Shim, M.; Pimparkar, N.; Alam, M. A.; Rotkin, S. V.; Rogers, J. A. *Nat. Nanotechnol.* **2007**, *2*, 230.
(29) Ding, L.; Yuan, D. N.; Liu, J. *J. Am. Chem. Soc.* **2008**, *130*, 5428.
(30) Dresselhaus, M. S.; Dresselhaus, G.; Saito, R.; Jorio, A. *Phys. Rep.* **2005**, *409*, 47.
(31) Lu, C. G.; Fu, Q.; Huang, S. M.; Liu, J. *Nano Lett.* **2004**, *4*, 623.
(32) Back, J. H.; Kim, S.; Mohammadi, S.; Shim, M. *Nano Lett.* **2008**, *8*, 1090.
(33) Qi, H.; Qian, C.; Liu, J. *Chem. Mater.* **2006**, *18*, 5691.
(34) Kong, J.; Cassell, A. M.; Dai, H. J. *Chem. Phys. Lett.* **1998**, *292*, 567.
(35) Lu, J.; Nagase, S.; Zhang, X. W.; Wang, D.; Ni, M.; Maeda, Y.; Wakahara, T.; Nakahodo, T.; Tsuchiya, T.; Akasaka, T.; Gao, Z. X.; Yu, D. P.; Ye, H. Q.; Mei, W. N.; Zhou, Y. S. *J. Am. Chem. Soc.* **2006**, *128*, 5114.
(36) Kocabas, C.; Kang, S. J.; Ozel, T.; Shim, M.; Rogers, J. A. *J. Phys. Chem. C* **2007**, *111*, 17879.

NL803496S